Electrical properties of InSb quantum wells remotely doped with Si

K. J. Goldammer,[a] W. K. Liu,[b] G. A. Khodaparast, S. C. Lindstrom, M. B. Johnson, R. E. Doezema, and M. B. Santos
Laboratory for Electronic Properties of Materials and Department of Physics and Astronomy, University of Oklahoma, Norman, Oklahoma 73019

(Received 22 December 1997; accepted 27 January 1998)

Two-dimensional electron systems were realized in InSb quantum wells with $Al_xIn_{1-x}Sb$ barrier layers δ-doped with Si. Measured electron mobilities in multiple-quantum-well structures were as high as 41 000 cm^2/V s at room temperature and 209 000 cm^2/V s at 77 K. Simple models can be used to explain the observed dependencies of the electron density on the quantum-well-to-dopant distance and on the number of quantum wells. Characterization by atomic force microscopy indicates that layer morphology may be a factor limiting electron mobility. © *1998 American Vacuum Society.* [S0734-211X(98)08603-X]

I. INTRODUCTION

The intrinsically high mobility of electrons in narrow-gap semiconductors makes InSb thin films attractive for magnetic-field sensing applications. At present, Te-doped InSb epilayers are paired with rare-earth metal magnets in automotive position-sensing applications where accuracy and repeatability are critical.[1] These devices exploit a geometrical magnetoresistance where sensitivity is proportional to mobility squared.[2] The 1.5 μm thick InSb layers are grown on GaAs substrates and have an electron concentration of 8×10^{16} cm^{-3} and a mobility of $\mu=40\,000$ cm^2/V s. The layers must be doped in order to reduce the temperature dependence of the electron concentration and, in turn, the temperature dependence of the sensor output. Unfortunately, the accompanying increase in ionized impurity scattering reduces the electron mobility and, consequently, the device sensitivity.

Remotely doped InSb quantum-well structures[3] are potentially better suited for magnetoresistance applications than uniformly doped InSb epilayers. Increased sensitivity is possible since a high mobility can be maintained while achieving a high extrinsic electron concentration. Also, the temperature dependence of the electron concentration can be reduced since only very thin layers of InSb are required. In this article, we report on the electrical properties of InSb multiple-quantum-well structures grown by molecular beam epitaxy on GaAs(001) substrates. Mobilities up to 41 000 cm^2/V s at room temperature and 209 000 cm^2/V s at 77 K are observed in Hall-effect measurements. Although the room-temperature mobility is the same as in the uniformly doped InSb mentioned above, the electron concentration in the quantum wells, 2.4×10^{17} cm^{-3}, is several times larger. Morphological characterization by atomic force microscopy indicates that roughness at the well/barrier interfaces may be a factor limiting the electron mobility. Increases in both the mobility and the electron concentration are anticipated from modifications to the layer structure.

[a]Electronic mail: kjgoldam@mail.nhn.ou.edu
[b]Current address: Quantum Epitaxial Designs, Inc., 119 Technology Drive, Bethlehem, PA 18015.

II. EXPERIMENT

All $InSb/Al_xIn_{1-x}Sb$ growths were performed in an Intevac Modular Gen II molecular beam epitaxy system. Effusion cells were loaded with In (7N RASA), Al (6N Ulvac), Sb (6.5N Dowa), and Si (Silicon Sense). An EPI Sb cracker was used with a cracking zone temperature of 900 °C. Growth rates for InSb and AlSb were calibrated and $Al_xIn_{1-x}Sb$ composition was deduced from temporal oscillations in the intensity of the reflection high-energy electron diffraction (RHEED) pattern and verified through high-resolution x-ray diffraction. An $Al_xIn_{1-x}Sb$ alloy composition with $x=0.09$ was maintained to keep the lattice mismatch to InSb below ~0.5% while allowing for a sufficiently large barrier for the electrons in the quantum wells.[4] The Sb-to-group-III flux ratio was slightly larger than unity with an InSb growth rate of ~0.8 ML/s. Delta doping was performed under an Sb flux and at a Si cell temperature of 1273 °C [$\sim5.3\times10^{11}$ net donor atoms cm^{-2} s^{-1}]. Substrate temperatures were calibrated through changes in the static (Sb flux only) RHEED pattern upon crossing the transition temperature $T_{tr}\sim390$ °C, at which the $Al_xIn_{1-x}Sb$ surface reconstruction changes between $c(4\times4)$ and pseudo-(1×3).[5]

The layer structure describing all the samples studied is shown in Fig. 1.[6] Growth was carried out on semi-insulating GaAs(001) substrates in order to eliminate electrical conduction through the substrate. Since the lattice constant of GaAs is ~14% smaller than that of InSb and $Al_xIn_{1-x}Sb$, a 1 μm buffer layer of AlSb, which has an intermediate lattice constant, was grown directly on the GaAs substrate.[7] A 1 μm thick $Al_xIn_{1-x}Sb$ layer was grown next, then followed by a ten-period 25-Å-$Al_xIn_{1-x}Sb$/25-Å-InSb strained-layer superlattice for dislocation filtering and surface smoothing. A 3 μm $Al_xIn_{1-x}Sb$ buffer layer was grown to promote full lattice relaxation as well as to isolate the carriers from scattering centers associated with this relaxation. The $Al_xIn_{1-x}Sb$ buffer layer was grown at $T_{tr}+50\pm5$ °C, since growth on a pseudo-(1×3), as opposed to $c(4\times4)$, surface reconstruction results in better pseudomorphic growth.

Electrons are supplied to each strained InSb quantum well

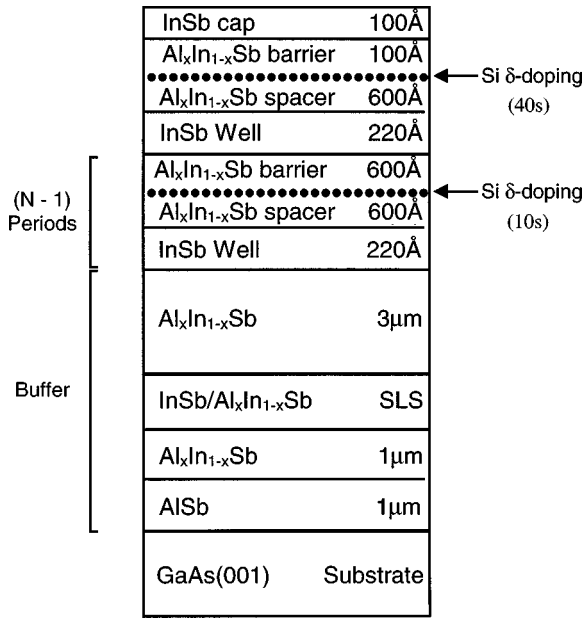

FIG. 1. Layer sequence for the remotely doped quantum-well structures.

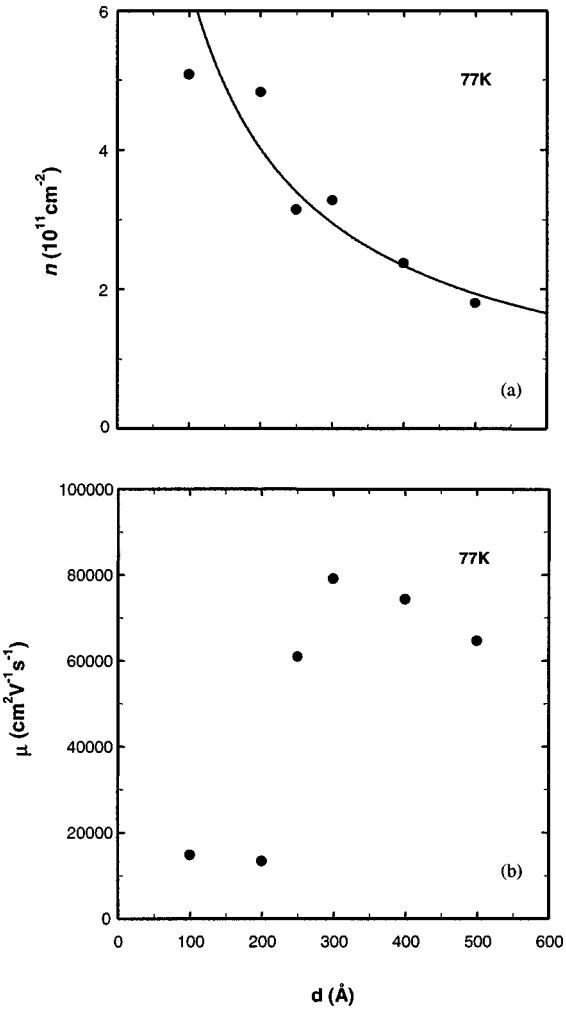

FIG. 2. Measured electron (a) density and (b) mobility in single-quantum-well structures at 77 K. The solid line in (a) shows the prediction of a simple electrostatic model.

by Si δ-doped layers [$\sim 5\times10^{11}$ cm^{-2} net donor density] in adjacent $Al_xIn_{1-x}Sb$ barriers. Each of the N quantum wells is 220 Å thick, which is below the Matthews and Blakeslee critical thickness.[8] All layers following and including the last 0.1 μm of the $Al_xIn_{1-x}Sb$ buffer layer were grown at a substrate temperature of $T_{tr}-30\pm5$ °C in order to minimize Si compensation.[9] Additional Si atoms were included in the δ-doped layer nearest to the surface in order to provide $\sim 2\times10^{12}$ cm^{-2} electrons for surface states. An InSb cap was added to prevent possible oxidation of an $Al_xIn_{1-x}Sb$ surface.

Hall-effect measurements at magnetic fields up to 0.25 T were performed on square samples whose edges are $\sim$4 mm long. Electrical contact was made at each corner of a sample by alloying In at $\sim$230 °C in a H_2 (20%)/N_2 (80%) atmosphere for 5 min. Ohmic contact was checked through observation of linear current–voltage characteristics. Resistivity was determined from van der Pauw measurements at 300 and 77 K.[10]

After growth was completed, samples were scanned in air using a Topometrix atomic force microscope running in noncontact phase mode. The high-resonant-frequency silicon tip had an aspect ratio of approximately 3:1 and a radius of curvature less than 200 Å.

III. RESULTS AND DISCUSSION

A. Spacer dependence in single-quantum wells

A series of six single-quantum-well structures ($N=1$) was grown with $Al_xIn_{1-x}Sb$ barrier layers sandwiching a 220 Å thick InSb quantum well. To provide electrons for the quantum well and surface states, a single Si δ-doped layer was placed in the upper $Al_xIn_{1-x}Sb$ barrier a distance 100 Å$\leqslant d\leqslant$500 Å above the InSb quantum well. Figure 2 shows the measured electron density n and mobility μ of the samples at 77 K.

A simple electrostatic model can be used to explain the observed dependence of electron density on spacer layer thickness:

$$\frac{qn}{\varepsilon}=\frac{E_b-E_F}{qd}, \tag{1}$$

$$n=\int_{E_0}^{E_F}\frac{m^*_{\text{edge}}}{\pi\hbar^2}\left(1+\frac{2E}{E_g}\right)dE. \tag{2}$$

Equation (1) describes the electric field in the spacer layer if background ionized impurities are ignored and the Fermi level at the δ-doped layer is pinned at the conduction-band edge. The well density at zero temperature is calculated in Eq. (2), assuming only a single subband is occupied and using the density of states determined from the two-band model. Values of $E_g\approx200$ meV for the band gap, $m^*_{\text{edge}}=0.0145m_0$ for the band-edge mass, and $\varepsilon=17.7\varepsilon_0$ for the dielectric constant are appropriate for InSb. The barrier height $E_b=142$ meV was deduced by assuming that 85% of

the InSb/$Al_xIn_{1-x}Sb$ band-edge discontinuity appears in the conduction band. In calculating the subband energy $E_0 = 24$ meV, strain and the nonparabolic dispersion relation were taken into account but the effects of band bending were ignored. Equations (1) and (2) can be combined to express n as a function of d. The results of this calculation are shown as a solid line in Fig. 2(a). Although in good agreement with the data, uncertainties in E_F at the δ-doped layer, E_b (due to the unknown value of the conduction-band offset), and E_0 (due to neglecting band bending) may still be important.

The dependence of μ and d [Fig. 2(b)] reveals the strong effect of remote ionized dopant scattering. Since n is much less than the net donor density provided by the single δ-doped layer, the majority of donor electrons must reside in surface states. As will be shown below, an improvement in mobility was observed in multiple-quantum wells where most of the electrons in the wells are far from the heavily doped layer near the surface.

B. Dependence on number of quantum wells

A series of multiple-quantum-well structures ($1 \leqslant N \leqslant 14$) was grown in which the only parameter intentionally varied was the number of quantum wells. The distance from each dopant layer to the nearest quantum well was $d = 600$ Å. The room-temperature and 77 K values for n and μ are shown in Fig. 3. The dependencies on N result from the increasing importance of conduction through the quantum wells with increasing N.

The filled circles in Fig. 3(a) show that n at 77 K is linearly proportional to the number of filled quantum wells. When a quantum well is remotely doped on both sides, the left-hand side of Eq. (1) must be divided by 2. Consequently, the electron density in the well closest to the substrate will be as predicted in Fig. 2, while the other $N-1$ wells will have densities that are 1.7 times greater. Therefore, the number of filled quantum wells is defined as $N-0.4$.[6] As in the previous section, we make the approximation that n at 77 K is due entirely to extrinsic electrons $N \times e_{\text{well}}$ that reside in the quantum wells but originate from Si dopants in the barrier layers. Hence, a value for e_{well} can be deduced from a line of best fit that also passes through the origin. The slope of such a line, shown in Fig. 3(a), gives $e_{\text{well}} = 3.5 \times 10^{11}$ cm^{-2}.

The density at room temperature is the sum of $N \times e_{\text{well}}$ plus the intrinsic densities in the quantum wells $N \times i_{\text{well}}$, the barrier layers $N \times i_{\text{bar}}$, and the buffer layers i_{buffer}. From the slope of a line fit to the room-temperature points and forced through i_{buffer} at the ordinate axis, a value of $e_{\text{well}} + i_{\text{well}} + i_{\text{bar}} = 4.5 \times 10^{11}$ cm^{-2} is determined. A value for i_{buffer} of 2.6×10^{11} cm^{-2} is determined from a Hall measurement on a structure with the quantum wells and barriers etched off. Since the band gap of AlSb is very large, i_{buffer} is assumed to be due entirely to electrons in the 4 μm $Al_xIn_{1-x}Sb$ layer. Multiplying i_{buffer} by a ratio of thicknesses (1200 Å/4 μm) yields an estimate of $i_{\text{bar}} = 0.8 \times 10^{10}$ cm^{-2}. A value for $i_{\text{well}} = 4.5 \times 10^{11}$ cm^{-2} $- 3.5 \times 10^{11}$ cm^{-2} $- 0.8 \times 10^{10}$ cm^{-2} $= 0.9 \times 10^{11}$ cm^{-2} can then be deduced. Dividing i_{well} by the well thickness of 220 Å yields a concentration of 4.2 $\times 10^{16}$ cm^{-2}, a value comparable to that measured in intrinsic InSb layers ($\sim 2 \times 10^{16}$ cm^{-2}). The consistency of the deduced values of i_{buffer}, i_{bar}, and i_{well} with measured values of $Al_xIn_{1-x}Sb$ and InSb layers is evidence for the validity of our model.

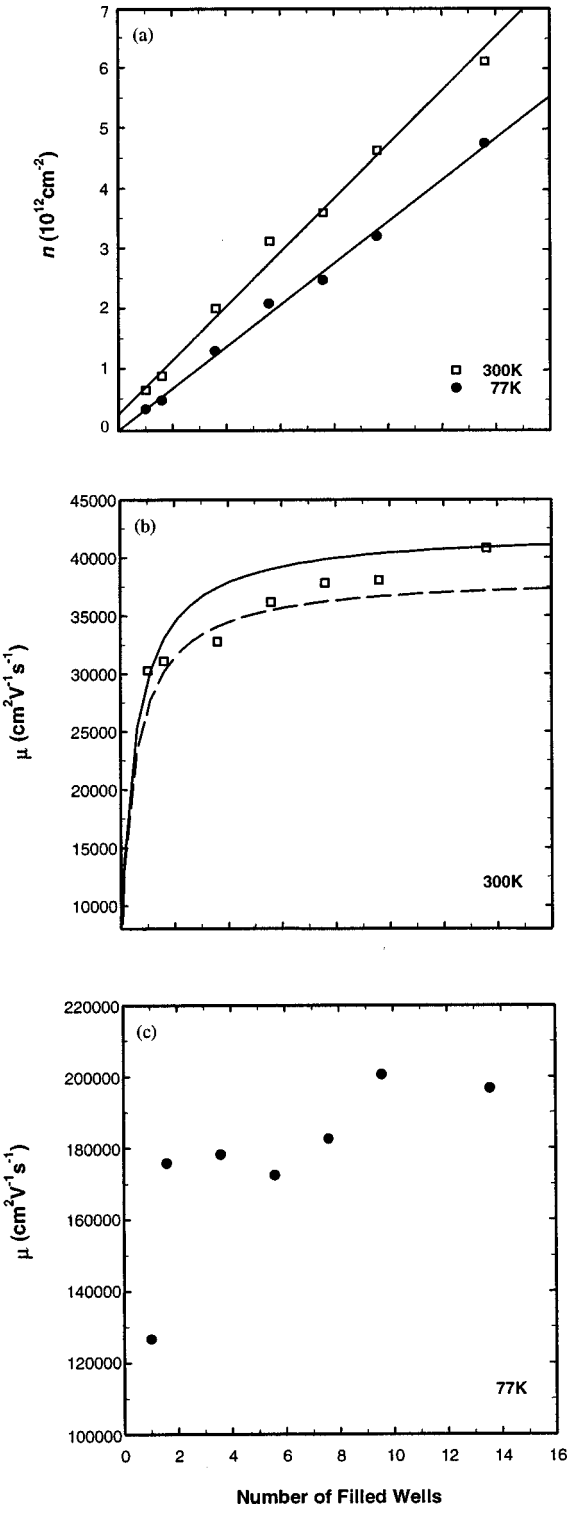

FIG. 3. Measured electron (a) density at room temperature and 77 K, (b) mobility at room temperature, and (c) mobility at 77 K. The solid lines in (a) are fits to the data with forced ordinate-axis intercepts.

The density values deduced above can be used to model the N dependence of the room-temperature mobility. As shown in Fig. 3(b), a trend toward higher mobility is evident with increasing N. As discussed above, an appreciable density of intrinsic carriers is present in the $Al_xIn_{1-x}Sb$ buffer and barrier layers at room temperature. As a result, the room-temperature transport behavior is expected to be a combination of both intrinsic electrons in the buffer, barrier, and wells, and extrinsic electrons in the wells. For the structure with $N=1$, the percentage of electrons that are extrinsic is $\sim 53\%$, the ratio between n at 77 K and n at room temperature. This percentage can be increased by growing structures with more periods. Each additional period adds a 220 Å thick quantum well, a Si δ-doped layer, and an additional $2\times d = 1200$ Å of $Al_xIn_{1-x}Sb$ barrier material. As deduced above, the density of resulting intrinsic carriers in the additional barrier material ($i_{bar}=0.8\times 10^{10}$ cm^{-2}) is much less than the density of additional electrons in the well ($e_{well}+i_{well}=4.4\times 10^{11}$ cm^{-2}). Because μ in InSb is higher than in $Al_xIn_{1-x}Sb$, the ratio of high-μ carriers to low-μ carriers, and consequently the measured μ, should be enhanced. As the number of quantum wells is increased, the percentage of extrinsic carriers increases to $\sim 78\%$ and the mobility increases to 41 000 cm^2/V s when $N=14$.

The mobility in an N-period multiple-quantum-well structure can be approximated as $\mu=(n_{alloy}\mu_{alloy}+n_{well}\mu_{well})/(n_{alloy}+n_{well})$, where $n_{alloy}=i_{buffer}+N\times i_{bar}$ is the density of electrons in the alloy layers, and $n_{well}=N\times(e_{well}+i_{well})$ is the density of electrons in the quantum wells. All the density values in this equation were determined as discussed above and a value of $\mu_{alloy}=8000$ cm^2/V s was measured in a 4 μm sample of $Al_xIn_{1-x}Sb$. Since all other necessary quantities are known, a value for μ_{well} can be deduced by a single-parameter curve fit to the data in Fig. 3(b). The data are bracketed between curves with μ_{well} set at 39 000 and 43 000 cm^2/V s. To the best of our knowledge, our measured value of 41 000 cm^2/V s is the highest room-temperature mobility reported in a quantum well made of any semiconductor, including InAs (Ref. 11) and GaAs. However, it is still significantly lower than the $\sim 60\,000$ cm^2/V s that we and others[12–14] observe in undoped InSb layers on GaAs substrates.

The measured mobilities at 77 K are shown in Fig. 3(c). A dramatic jump in μ occurs from 126 000 cm^2/V s for $N=1$ to 175 500 cm^2/V s for $N=2$. Increasing N results in only a slightly higher μ, with a maximum of 209 500 cm^2/V s for $N=10$. This is in contrast to the gradual increase in mobility observed at room temperature. Since virtually all of the carriers at this temperature are extrinsic electrons in the wells, one would expect the mobility to be independent of N. Although the causes of the anomalous low μ for $N=1$ are still under investigation, we believe that remote ionized dopant scattering plays a major role. The very high density of the doped layer closest to the surface would make the $N=1$ structure more limited by such scattering than structures with larger N.

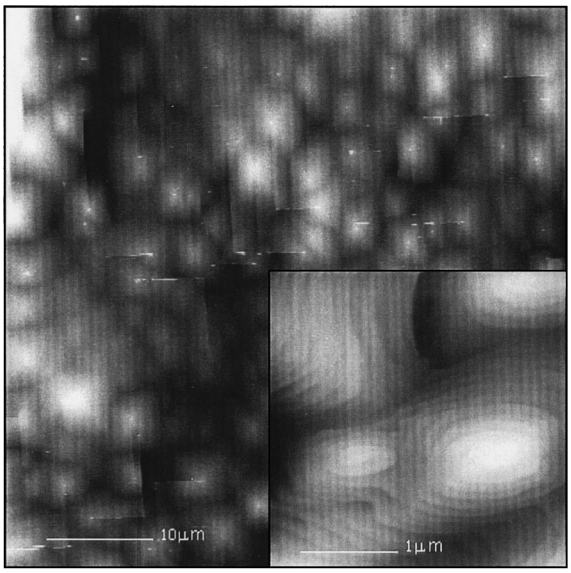

FIG. 4. Noncontact atomic force microscope images of a single-quantum-well sample. The large image is a 50 μm square region with the gray scale representing a height variation of 1000 Å. The small image (inset) is a 2.6 μm square region with the gray scale representing a height variation of 100 Å.

C. Atomic force microscopy

Atomic force microscopy was performed on many of the quantum-well structures. Figure 4 shows an atomic force micrograph of the $N=1$ structure with $d=600$ Å. The large-scale image reveals pyramidal features as well as abrupt steps oriented in the [110] and [1$\bar{1}$0] directions. The inset to Fig. 4 shows that these pyramidal features are actually spiral-like structures that grow around threading (screw) dislocations. The step heights on the pyramids correspond to 2 ML and the pyramid heights range from ~ 100 to ~ 500 Å with a characteristic separation of ~ 3 μm. The size and density of these features is similar in all of the quantum-well structures studied. However, the oriented abrupt steps are, typically, ~ 100 Å in height, 5–10 μm long, separated by ~ 5 μm, and, unlike the pyramidal features, are less numerous in the structures with $N>1$. This may be due to dislocation filtering occurring at the well/barrier interfaces of our $N>1$ structures.

These studies indicate that the morphology of the active layers may play a role in limiting the mobility of the electrons in the wells. Both the pyramidal and oriented abrupt steps cause thickness variations comparable to the well width (220 Å). Moreover, the spacing of these defects is on the same scale as the mean-free path of the electrons in the wells [$l=(\hbar/e)\mu_{well}(2\pi n_{well})^{1/2}\approx 0.4$ μm at room temperature] and will, therefore, adversely affect the mobility, particularly at low temperature. Therefore, the large variation in the number of oriented abrupt steps between the $N=1$ and $N>1$ structures may account in part for the anomalously low mobility in the $N=1$ sample at 77 K. Further microscopy studies are under way to test this conjecture and to optimize buffer layer design.

IV. CONCLUSIONS

In InSb quantum wells with $Al_xIn_{1-x}Sb$ barrier layers δ-doped with Si, room-temperature electron mobilities as high as 41 000 cm^2/V s were observed for electron concentrations of 2.4×10^{17} cm^{-3}. Even higher mobility should be possible with improved surface morphology and higher electron concentrations should result from decreasing the quantum-well-to-dopant distance.

ACKNOWLEDGMENTS

The authors would like to acknowledge Fred McKenna for technical assistance and Seokjae Chung for useful discussions. This work is supported by the Oklahoma Center for the Advancement of Science and Technology and by NSF Grant Nos. ECS-9410015, OSR-9550478, and DMR-9624699.

[1]J. P. Heremans, Mater. Res. Soc. Symp. Proc. **475**, 63 (1997).
[2]J. Heremans, D. L. Partin, C. M. Thrush, and L. Green, Semicond. Sci. Technol. **8**, S424 (1993).
[3]W. K. Liu, X. Zhang, W. Ma, J. Winesett, and M. B. Santos, J. Vac. Sci. Technol. B **14**, 2239 (1996).
[4]M. K. Saker, D. M. Whittaker, M. S. Skolnick, C. F. McConville, C. R. Whitehouse, S. J. Barnett, A. D. Pitt, A. G. Cullis, and G. M. Williams, Appl. Phys. Lett. **65**, 1118 (1994).
[5]G. M. Williams, C. R. Whitehouse, A. G. Cullis, N. G. Chew, and G. W. Blackmore, Appl. Phys. Lett. **53**, 1847 (1988).
[6]The layer sequence of the $N=1$ structure with $d=600$ Å is not described by Fig. 1. A second δ-doped layer (10 s) was added 600 Å below the quantum well.
[7]L. K. Li, Y. Hsu, and W. I. Wang, J. Vac. Sci. Technol. B **11**, 872 (1993).
[8]J. W. Matthews and A. E. Blakeslee, J. Cryst. Growth **27**, 118 (1974).
[9]M. B. Santos, W. K. Liu, R. J. Hauenstein, K. J. Goldammer, W. Ma, and M. L. O'Steen, Mater. Res. Soc. Symp. Proc. **450**, 97 (1997).
[10]L. J. van der Pauw, Philips Res. Rep. **13**, 1 (1958).
[11]N. Kuze, K. Nagase, S. Muramatsu, S. Miya, T. Iwabuchi, A. Ichii, and I. Shibasaki, J. Cryst. Growth **150**, 1307 (1995).
[12]P. E. Thompson, J. L. Davis, J. Waterman, R. J. Wagner, D. Gammon, D. K. Gaskill, and R. Stahlbush, J. Appl. Phys. **69**, 7166 (1991).
[13]J. R. Soderstrom, M. M. Cumming, J-Y. Yao, and T. G. Anderson, Semicond. Sci. Technol. **7**, 337 (1992).
[14]G. Singh, E. Michel, C. Jelen, S. Slivken, J. Xu, P. Bove, I. Ferguson, and M. Razeghi, J. Vac. Sci. Technol. B **13**, 782 (1995).